Soft Matter

Accepted Manuscript

This article can be cited before page numbers have been issued, to do this please use: X. Ma, F. Li, Z. Xie, M. Xue, Z. ZHENG and X. Zhang, *Soft Matter*, 2017, DOI: 10.1039/C6SM02791A.

ROYAL SOCIETY OF CHEMISTRY

rsc.li/soft-matter-journal

View Article Online
DOI: 10.1039/C6SM02791A

Soft Matter

COMMUNICATION

Size-Tunable, Highly Sensitive Microelectrode Arrays Enabled by Polymer Pen Lithography

Received 00th January 20xx,
Accepted 00th January 20xx

DOI: 10.1039/x0xx00000x

www.rsc.org/

Xinlei Ma,[a] Fengwang Li,[b] Zhuang Xie,[c] Mianqi Xue,[b] Zijian Zheng,[c*] and Xueji Zhang[a*]

By combining polymer pen lithography (PPL) patterning with in-situ polymerization, we report a straightforward and bottom-up approach for bench-top fabrication of microelectrode arrays (MEAs) with well-controlled dimensions. The as-fabricated MEAs can be used to in-situ electrodeposit prussian blue and work as a biosensor for H_2O_2 with a detect limit as low as 5 nM at the sensitivity of 0.7 A cm^{-2} M^{-1}.

MEAs have been receiving significant attention in biological analysis, environmental monitoring, food safety, and disease diagnosis[1] for their unique electrochemical properties such as highly sensitive, small capacitive-charging currents, reduced iR drop(potential drop due to solution resistance), improved signal-to-noise ratio and current response, and steady-state diffusion currents.[2] As a general rule, with the size down to micrometer level, the size-effect can enhance the observed electrochemical response through adjusting the mass transport of redox active species to and from the electrode surface. MEA is capable of outputting satisfactory current response signals while overcoming the drawback of a single microelectrode having extremely large current densities yet very small absolute currents. Moreover, MEAs create an attractive and important opportunity for the integration of living, biological systems into lab-on-a-chip devices owing to their feasibility in sensing multiple analytes (via fabricating devices with individually addressable MEAs) and probing signal transmission.[3,4] Such advantages are very important for in-vitro or in-vivo biological applications such as enzyme-linked assays and the detection of many other biomolecules.

So far, various types of MEAs have been introduced to electrochemical analysis such as planar or recessed micro-disk electrode arrays, interdigitated microelectrode arrays,[5] regioselectivity electrode arrays,[6] micro-band electrode arrays,[7] linear microelectrode arrays,[8] and 3D microelectrode arrays.[9] These microstructured electrodes are usually manufactured by conventional lithographic techniques such as photolithography (for metal, carbon, and other electrode arrays),[10] screen-printing techniques,[11] direct electrodeposition[12] or unconventional methods such as assembly techniques[13] and soft lithography.[14] Besides, we have manufactured different functional micro structures by means of soft lithography,[15] microfluidic etching[16] and direct pen writing.[17] Those methods have their advantages respectively when it comes to the fabrication of MEAs. While these MEAs have been previously demonstrated to be very sensitive for the detection of biologically important species, fabrication of new types of MEAs with high resolution and controlled architecture in a simple and scalable way is still highly desired for the integration into microelectronic and microfluidic systems towards addressable MEA and multiplex detection.

Polymer-pen lithography (PPL), a molecular printing method developed in 2008, has been extensively exploited for mask-free and high-throughput fabrication of complex patterned nanostructures,[18] which combines the attributes of soft lithography[19] and dip-pen nanolithography (DPN)[20] into a single lithographic platform. This technique uses massive cantilever-free pyramidal pen arrays to direct deposit molecular materials onto a surface over cm^2 area, with precise size and registration control across nano to macro length scales by a scanning probe system.[18,21] Importantly, feature size ranging from 40 nm to over 10 µm can be easily adjusted through controlling patterning parameters (contact force, time, etc.) as well as external conditions (humidity, light etc.) in a single patterning experiment.[18,22,23] Compared with other techniques based on premade masks or templates such as soft lithography,[6,23a] colloidal lithography[23b] and subtractive patterning via lift off,[7,23c] in-situ growth,[23d] the ability to produce arbitrary, uniform patterns over macroscopic areas makes PPL an attractive tool for customized and bench-top device fabrication.

[a] Research Center for Bioengineering and Sensing Technology, Beijing Key Laboratory for Bioengineer and Sensing Technology, School of Chemistry and Biological Engineering, University of Science & Technology Beijing, 100083，Beijing, P. R. China. E-mail: zhangxueji@ustb.edu.cn
[b] Institute of Physics and Beijing National Laboratory for Condensed Matter Physics, Chinese Academy of Sciences, Beijing 100190, China.
[c] Nanotechnology Center, Institute of Textiles and Clothing, The Hong Kong Polytechnic University, Hung Hom, Kowloon, Hong Kong SAR, China. E-mail: tczzheng@polyu.edu.hk

View Article Online
DOI: 10.1039/C6SM02791A

Herein, by combining PPL patterning with in-situ polymerization, we report a straightforward and bottom-up approach to bench-top fabrication of MEAs with well-controlled dimensions. We firstly patterned 16-mercaptohexadecanoic acid (MHA) onto an Au-coated substrate by PPL as molecular resist, followed by passivation of the background with densely grown PMMA brushes through surface-initiated atom transfer radical polymerization (SI-ATRP). MEAs were then produced by simply plasma removing the MHA self-assembled monolayer (SAM) to expose the underlying Au surface. Further electrode modification with prussian blue (PB) was also demonstrated and the modified MEAs can function as electrochemical detector for H_2O_2, which plays an important role in the biological processes. Notably, MEAs with varied size and density can be easily produced in a programmable manner by adjusting the lithography parameters to screen their electrochemical performance. This method could allow rapid prototyping of functional electrochemical devices for various purposes.

Experimental Section

Fabrication of MEAs by polymer pen lithography

The MEAs were fabricated on an Au substrate as schematically shown in Fig. 1. The Au-coated n-doped Si wafer (5 nm Cr, 50 nm Au) was cleaned by ultrasonication in DI water, acetone, and isopropanol, sequentially, and was blown dry with N_2 prior to patterning procedure. Polymer pen arrays were fabricated following previously reported procedures.[24] The as-made polymer pen array was plasma-treated for 1 min and dipped into an ethanol solution of MHA (5 mM) and dried in air for inking. The inked polymer pen array was then mounted onto a customized z-piezo scanner (XE-100, Park Systems) and aligned to the plane of the Au substrate. After leveling, the pen array was programmed to contact with the substrate to write MHA patterns at ~30% relative humidity and room temperature (RT) with a dwell time of 0.5 s. Finally, the MHA-patterned substrate was backfilled with 1 mM ω-mercaptoundecyl bromoisobutyrate (MUDBr) ethanol solution and rinsed with fresh ethanol.

PMMA brushes were then grown on the substrate through surface-initiated atom transfer radical polymerization (SI-ATRP) in aqueous media:[25] the MUDBr-coated Au substrate was placed in Schlenk tubes under a N_2 atmosphere at around 35–40 °C, followed by adding the degassed monomer solution. Typically, the monomer solution used to prepare PMMA brushes is composed of 5 g MMA, 4 mL of methanol, 1 mL of DI water, Cu(I)Br (0.071 g), 2,2-dipyridyl (0.156 g). The polymerization time was varied from 0.5 to 8 h to control thickness. The determination of the optimum thickness of the PMMA layer is shown in supporting information (Fig. S2). After reaction, the resultant substrates were rinsed extensively with methanol, DI water and toluene, and then dried under a stream of N_2. Then the as-fabricated Au substrate was exposed to plasma for 30 s to remove the MHA and form Au MEAs.

Fabrication of Prussian Blue (PB)-Based MEAs

PB was electrochemically deposited onto the Au MEAs in 0.1 M hydrochloric acid containing 4 mM $K_3Fe(CN)_6$, 4 mM $FeCl_3$, and 0.1 M KCl with cyclic voltammetry. The electrode was scanned from -0.2 to +0.6 V (vs. Ag/AgCl, all potentials hereafter are with respect to this reference) for 3 cycles at the scan rate of 50 mV s^{-1}. The same procedures were applied for the fabrication of the Au/Cr/Si macroelectrode for the control experiments.The characterization of Prussian Blue deposited on the microelectrodes is shown in supporting information (Fig. S1).

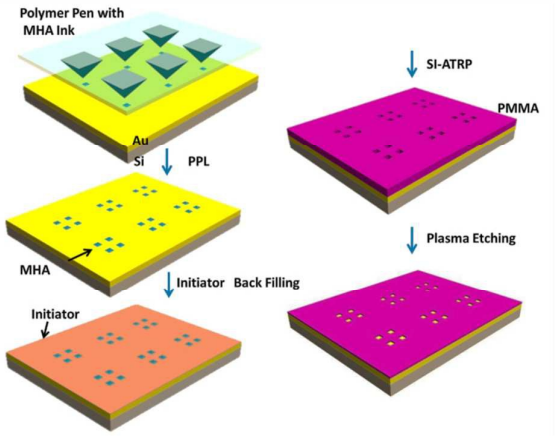

Fig. 1 Schematic procedure of fabricating the MEAs by polymer pen lithography.

Measurement

The optical photograph was taken by optical microscope Eclipse Ni (Nikon). Atomic force microscopy (AFM) were performed using an XE-100 (Park Systems). Plasma experiments were carried out by a plasma degumming machine PDC-32G (Harric Plasma). Electrochemical experiments were conducted in a standard three-electrode cell at room temperature using a computer-controlled CHI 660B electrochemical analyzer (CH Instruments, Shanghai Chenhua Instrument Corporation, China) and 1252A Frequency Response Analyzer (Solartron Analytical). A Pt spiral wire and an Ag/AgCl (saturated with KCl) were used as counter and reference electrodes, respectively. The Au MEAs and a piece of Au/Cr/Si substrate (macroelectrode) were used as working electrode for the voltammetric measurements. The electrode area of the MEAs was calculated using the area of exposed Au.

Results and Discussion

The MEAs were written on the Au/Cr/Si substrate originally by PPL with the MHA ink, as shown in Fig. 1. The PPL method offers the advantage in the ease of tuning the microelectrode geometry and array density. One can tune the microelectrode pitch sizes to create a pattern array geometry that exhibits microelectrode behavior while maximizing the number of microelectrode openings. The as-fabricated MHA arrays work as the mask in the initiator back filling process. In the following

View Article Online
DOI: 10.1039/C6SM02791A

SI-ATRP process, PMMA brush film grew on the Au surface where the initiator is present. To get rid of the loosely attached PMMA on the MHA protected area during the SI-ATRP process and the residual MHA, the substrate was exposed to plasma to get the MEAs.

Given to the shape of the tip used in PPL process, the shape of the individual microelectrode in the MEAs are square. The as-fabricated MEAs are shown in Fig. 2. The distance between the individual electrodes are 5μm (Fig. 2a), 8 μm (Fig. 2b) and 20 μm (Fig. 2c), and the corresponding side length of the square-shaped electrodes are 3.1±0.2 μm, 2.8±0.5 μm, 3.0±0.3 μm, respectively. The bright dots at the right up of each MEAs are the approaching dots during the PPL procedure. The MEAs are further investigated by AFM. As shown in Fig. 3, the width of the individual electrode is 3μm with an inter-electrode spacing of 5 μm, 8 μm and 20 μm, respectively, which is in consistent with the optical image results. The depth of electrode holes is 20±2 nm for all three electrodes.

Cyclic voltammetry (CV) is usually used to assess the properties of an electrode. The microelectrode arrays in CV measurement will have steady-state responses if the hemispherical diffusion layers of the individual microelectrodes are not perturbed by the adjacent microelectrodes.[26] Whereas once the diffusion layers overlap, which is known as shielding effect, peak-shaped CVs with smaller current densities are observed. On conditions that the center-to-center distance between two adjacent microelectrodes in an array is too small or too large, the unique features of MEAs will vanish and function as macroelectrode or an individual microelectrode, respectively. Consequently, the selection of an optimal microelectrode density in an array is important.

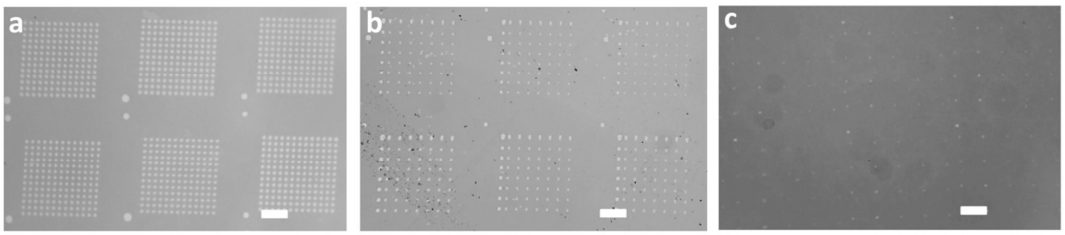

Fig. 2 The optical images of the as-fabricated MEAs at different densities, a) 3.1±0.2 μm width of individual electrode at a distance of 5 μm, b)2.8±0.5 μm width of individual electrode at a distance of 8 μm, c) 3.0±0.3 μm width of individual electrode at a distance of 20 μm. The scale bar is 20 μm.

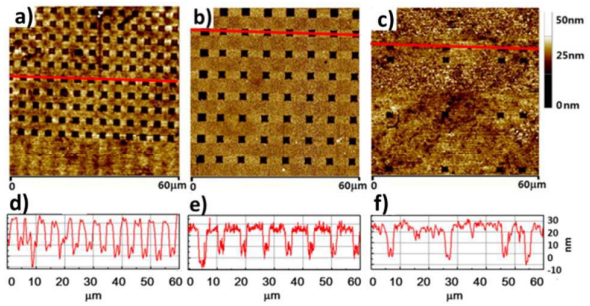

Fig. 3 The AFM images of the as-fabricated MEAs at different density, the width of individual electrode si about 3 μm in those three MEAs. a) individual electrode at a distance of 5 μm and d) the profile of the cross line, b) individual electrode at a distance of 8 μm and e) the profile of the cross line, c) individual electrode at a distance of 20 μm and f) the profile of the cross line.

To examine whether our fabricated MEAs possess the microelectrode behavior, CV characterization was done using 2.5 mM $Fe(CN)_6^{3-/4-}$ in 0.1 M KCl.

At Au macroelectrode, one pair of well-defined and peak-shaped redox wave was obtained at +0.23 V (Fig. 4a), which was ascribed to the electron transfer process of $Fe(CN)_6^{3-/4-}$ at this electrode.[27] The cathodic peak currents increase with increasing potential scan rate and were linear with the square root of the scan rate within the range from 10 to 100 mV s^{-1}, suggesting a diffusion-controlled feature of the redox process of $Fe(CN)_6^{3-/4-}$ at the electrode.[28] When the spacing is increased from 5 μm to 20 μm, the depletion zone in the CV reduces and a classic sigmoidal shaped CV emerges as the

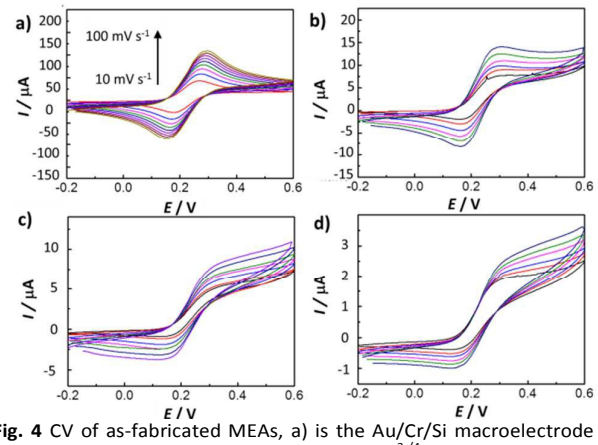

Fig. 4 CV of as-fabricated MEAs, a) is the Au/Cr/Si macroelectrode in 0.1 M KCl solution containing 2.5 mM $Fe(CN)_6^{3-/4-}$ with a scan rate of 10 to 100 mV s^{-1} (from inner to outside), b) 3 μm width of individual electrode at a distance of 5 μm, c) 3 μm width of individual electrode at a distance of 8 μm, d) 3 μm width of individual electrode at a distance of 20 μm in 0.1 M KCl solution containing 2.5 mM $Fe(CN)_6^{3-/4-}$.

sensors transit from macroelectrode to microelectrode behavior. At the spacing of 5 μm (Fig. 4b), the diffusion hemispheres of the individual microelectrodes overlap and give a peak-shaped CV. At the spacing of 8 μm (Fig. 4c), the CV obtained at the Au MEA exhibits a quasi-sigmoidal shape at

View Article Online
DOI: 10.1039/C6SM02791A

scan rate of 100 mV s^{-1}, implying the partial overlapping of the diffusion zones. At a spacing of 20 µm, the overlap of diffusion hemispheres of the individual microelectrodes continue to decrease as evidenced by the quasi-sigmoidal CV shape in Fig. 4d. This indicates that MEA with individual electrode in 3 µm width seperated by 20 µm can substantially deliever microelectrode features.

Davies and Compton[29] has put forward a function to describe the design criterion for an effective MEA.

$$d>2\sqrt{2D\frac{\Delta E}{v}} \quad (1)$$

Where ΔE is the potential range from the foot of the forward wave to the reverse point and v is the potential scan rate, and D is the diffusion coefficient (7.6×10^{-6} cm^2 s^{-1} for $Fe(CN)_6^{3-}$).However, according to the formula 1, in the $Fe(CN)_6^{3-/4-}$ system at the scan rate of 100 mV s^{-1}, the distance between the individual should be 135 µm, which is larger than 20 µm in our case. This indicates the as-fabricated Au arrays does not behaviour as a perfect MEA, where "the distance between neighbouring microelectrodes is large enough such that there is no overlapping of diffusion zones and the diffusion domain response is identical to the response of the individual microelectrode".[29] The diffusion layer of each microelectrode overlaps with that of adjacent microelectrodes to some extent and the MEAs have the mixture electrochemical behaviour of 1D linear diffusion and 2D radial diffusion. Our MEAs perform like a "quasi microelectrode"[29] and the overlap is not substantially significant to make the MEAs behaviour like a macro electrode. The minimum distance between the neighboring electrode is sufficient at 20 µm in the PPL fabricated MEAs system. As long as the geometry for the MEA has a sufficient spacing and the device would operate in a microelectrode array system. All MEAs were fabricated using 20 µm spacing.

The electrochemical performance of an Au macroelectrode was compared to the as-fabricated MEA device, using H_2O_2 as the analyte (Fig. 5). The electrochemical deposition PB was first modified on the surface of the MEA device, with the extraordinary electrochemical properties in the electrocatalytic process. Sensitive measurement of H_2O_2 is of great importance both in biological studies and in the development of electrochemical biosensors since, as one kind of reactive oxygen species, H_2O_2 plays a great role in the biological processes.[30] The acceleration of H_2O_2 reduction at a potential more positive than O_2 reduction becomes essential since the slow kinetics in the redox process of H_2O_2 leads to a high potential for the oxidation and a low potential of the reduction, resulting in the interference from, for example, ascorbic acid and O_2.[31] PB is our choice to work as "artificial peroxidase" since it's the most effective electrocatalyst for the H_2O_2 reduction among almost all kinds of electrocatalysts reported so far.[32] At Au macroelectrode, well defined current responses were recorded with successive addition of H_2O_2 into 0.1 M phosphate buffer (pH 7.4). The sensitivity for H_2O_2 was enhanced at the as-fabricated MEAs (i.e., 0.7 A cm^{-2} M^{-1}), as compared with that at the Au macroelectrode (i.e., 0.4 A cm^{-2} M^{-1}, as shown in the inset of Fig. 5). The enhancement basically benefits from the electrochemical character of MEA. Moreover, the detection limit obtained at the MEAs is down to 5 nM which is 20 times lower than that obtained at the Au macroelectrode (100 nM). The excellent analytical properties of MEAs substantially enable its applications both for the detection of H_2O_2 and for the development of highly sensitive electrochemical biosensors.

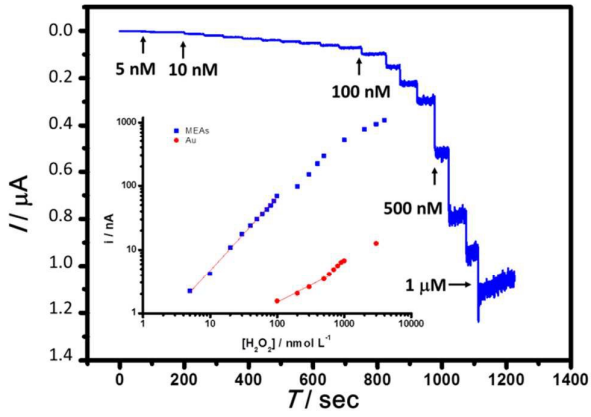

Fig.5 Amperometric responses observed at PB based MEA with distance of 20µm spacing among adjacent electrodes in 0.1 M phosphate buffer (pH 7.4) applied -0.1 V vs Ag/AgCl upon successive addition of H_2O_2. The amount of H_2O_2 added each time ranges from 5 to 1000 nM as indicated. The inset plot shows the relationship between the amperometric current density and the concentration on PB based Au MEA (blue dots) and Au/Cr/Si macroelectrode (red dots) of H_2O_2 within the range 5×10^{-9} to 4×10^{-6} M.

Conclusions

A microelectrode array sensor has been successfully fabricated by a bottom-up approach based on PPL and in-situ polymerization. With PPL patterning, the size of individual electrode and the spacing between neighboring electrodes can be fine controlled. This allows screening of microelectrode behavior in the electro-analytical system and the optimization of size parameters. The as-fabricated MEAs can be readily applied in the sensing of bioanalytes such as H_2O_2 after electrodeposition of Prussian blue, which exhibits high sensitivity and ultralow detection limit. This simple and rapid approach will allow low-cost and customized fabrication of MEAs with excellent electrochemical performance for various electroanalytical applications. In addition, with multiplexed patterning techniques enabled by the polymer pen arrays,[33] complicated and integrated devices could be envisioned for combinatorial and high-through put analysis.[22f,34]

Acknowledgements

This research was supported by National Natural Science Foundation of China 21404009, Beijing Natural Science Foundation 2154053, Fundamental Research Funds for the Central Universities FRF-TP-15-020A2, Grand from Beijing

View Article Online
DOI: 10.1039/C6SM02791A

Municipal Science and Technology Commission z131102002813058

Notes and references

1. (a) Z. Lin, Y. Takahashi, T. Murata, M. Takeda, K. Ino, H. Shiku and T. Matsue, *Angew. Chem. Int. Ed.*, 2009, **48**, 2044-2046; (b) C. Y. Lee, Y. J. Tan and A. M. Bond, *Anal. Chem.*, 2008, **80**, 3873-3881; (c) R. Feeney and S. P. Kounaves, *Electroanal.*, 2000, **12**, 677-684; (d) M. J. Li, Y. Sato, S. Nishizawa, T. Seino, K. Nakamura and N. Teramae, *J. Am. Chem. Soc*, 2009, **131**, 2448-2449.
2. H. P. Wu, *Anal. Chem.*, 1993, **65**, 1643-1646.
3. C. Xie, J. Liu, T. M. Fu, X. C. Dai, W. Zhou and C. M. Lieber, *Nat. Mater.*, 2015, **14**, 1286-1292.
4. (a) A. Canales, X. T. Jia, U. P. Froriep, R. A. Koppes, C. M. Tringides, J. Selvidge, C. Lu, C. Hou, L. Wei, Y. Fink and P. Anikeeva, *Nat. Biotechnol.*, 2015, **33**, 277-284; (b) J. Lee, I. Ozden, Y.-K. Song and A. V. Nurmikko, *Nat. Methods.*, 2015, **12**, 1157-1162; (c) Y. Zhang, H. Wang, J. F. Nie, Y. W. Zhang, G. L. Shen, R. Q. Yu, *Biosens. Bioelectron.*, 2009, **25**, 34-40.
5. A. E. Cohen and R. R. Kunz, *Sensor. Actuat. B-Chem.*, 2000, **62**, 23-29.
6. F. W. Li, M. Q. Xue, X. L. Ma, M. N. Zhang and T. B. Cao, *Anal. Chem.*, 2011, **83**, 6426-6430.
7. J. C. He, X. L. Ma, Y. H. Zhu, F. W. Li, X. F. Tang, X. G. Zhang and M. N. Zhang, *Electrochem. Commun.*, 2013, **30**, 67-70.
8. L. J. Magee Jr and J. Osteryoung, *Anal. Chem.*, 1989, **61**, 2124-2126.
9. G. Charvet, L. Rousseau, O. Billoint, S. Gharbi, J. P. Rostaing, S. Joucla, M. Trevisiol, A. Bourgerette, P. Chauvet and C. Moulin, *Biosens. Bioelectron.*, 2010, **25**, 1889-1896.
10. (a) S. Y. Hwang, H. H. Park, S. M. Kang, H. B. Shin and H. K. Kang, *Thin Solid Films*, 2013, **546**, 132-135; (b) O. J. Schueller, S. T. Brittain and G. M. Whitesides, *Sensor. Actuat. A-Phys.*, 1999, **72**, 125-139.
11. M. Dequaire and A. Heller, *Anal. Chem.*, 2002, **74**, 4370-4377.
12. A. N. Bezbaruah and T. C. Zhang, *Anal. Chem.*, 2002, **74**, 5726-5733.
13. M. Riepl, V. M. Mirsky and O. S. Wolfbeis, *Microchim. Acta.*, 1999, **131**, 29-34.
14. D. Qin, Y. Xia and G. M. Whitesides, *Nat. Protoc.*, 2010, **5**, 491-502.
15. (a) X. L. Ma, D. Zhao, M. Q. Xue, H. Wang and T. B. Cao, *Angew. Chem. Int. Ed.*, 2010, **49**, 5537-5540; (b) D. Zhao, L. T. Duan, M. Q. Xue, W. Ni and T. B. Cao, *Angew. Chem. Int. Ed.*, 2009, **48**, 6699-6703; (c) M. Q. Xue, Y. H. Yang and T. B. Cao, *Adv. Mater.*, 2008, **20**, 596-600; (d) M. Q. Xue, Y. Wang, X. W. Wang, X. C. Huang and J. H. Ji, *Adv. Mater.*, 2015, **27**, 5923-5929.
16. M. Q. Xue, Z. Xie, L. S. Zhang, X. L. Ma, X. L. Wu, Y. G. Guo, W. G. Song, Z. B. Li and T. B. Cao, *Nanoscale*, 2011, **3**, 2703-2708.
17. M. Q. Xue, D. Chen, Y. J. Long, P. P. Wang, L. X. Zhao and G. F. Chen, *Adv. Mater.*, 2015, **27**, 3614-3619.
18. F. W. Huo, Z. J. Zheng, G. F. Zheng, L. R. Giam, H. Zhang and C. A. Mirkin, *Science*, 2008, **321**, 1658-1660.
19. Y. Xia and G. M. Whitesides, *Angew. Chem. Int. Ed.*, 1998, **37**, 550-575.
20. R. D. Piner, J. Zhu, F. Xu, S. H. Hong and C. A. Mirkin, *Science*, 1999, **283**, 661-663.
21. (a) Z. Xie, Y. D. Shen, X. C. Zhou, Y. Yang, Q. Tang, Q. Miao, J. Su, H. K. Wu and Z. J. Zheng, *Small*, 2012, **8**, 2664-2669; (b) M. Q. Xue, X. J. Cai and G. F. Chen, *Small*, 2014, **11**, 548-552; (c) Z. Xie, C. J. Chen, X. C. Zhou, T. T. Gao, D. Q. Liu, Q. Miao and Z. J. Zheng, *ACS Appl. Mater. Interface*, 2014, **6**, 11955-11964.
22. (a) X. Liao, A. B. Braunschweig, Z. J. Zheng and C. A. Mirkin, *Small*, 2010, **6**, 1082-1086; (b) Y. Zhou, Z. Xie, K. A. Brown, D. J. Park, X. Z. Zhou, P. C. Chen, M. Hirtz, Q. Y. Lin, V. P. Dravid, G. C. Schatz, Z. J. Zheng and C. A. Mirkin, *Small*, 2015, **11**, 913-918; (c) D. J. Eichelsdoerfer, K. A. Brown, M. X. Wang and C. A. Mirkin, *J. Phys. Chem. B*, 2013, **117**, 16363-16368; (d) Z. Xie, Y. Zhou, J. L. Hedrick, P. C. Chen, S. He, M. M. Shahjamali, S. Z. Wang, Z. J. Zheng and C. A. Mirkin, *Angew. Chem. Int. Ed.*, 2015, **54**, 12894-12899; (e) L. R. Giam, M. D. Massich, L. Hao, L. S. Wong, C. C. Mader and C. A. Mirkin, *Proc. Natl. Acad. Sci. U.S.A.*, 2012, **109**, 4377-4382; (f) L. R. Giam, M. D. Massich, L. Hao, L. S. Wong, C. C. Mader and C. A. Mirkin, *Proc. Natl. Acad. Sci. U.S.A.*, 2012, **109**, 4377-4382.
23. (a) C. Q. Ye, M. Z. Li, M. Q. Xue, W. Shen, T. B. Cao, Y. L. Son and L. Jiang, *J. Mater. Chem.*, 2011, **21**, 5234-5237; (b) S.g-M. Yang, S. G. Jang, D.-G. Choi, S. Kim and H. K. Yu, *Small*, 2006, **2**, 458–475; (c) W.-S. Liao, S. Cheunkar, H. H. Cao, H. R. Bednar, P. S. Weiss and A. M. Andrews, *Science*, 2012, **337**, 1517-1521; (d) M. Q. Xue, F. W. Li, Y. Wang, X. Cai, F. Pan and J. T. Chen, *Nanoscale*, 2013, **5**, 1803-1805.
24. D. J. Eichelsdoerfer, X. Liao, M. D. Cabezas, W. Morris, B. Radha, K. A. Brown, L. R. Giam, A. B. Braunschweig and C. A. Mirkin, *Nat. Protocols*, 2013, **8**, 2548-2560.
25. D. M. Jones, A. A. Brown and W. T. S. Huck, *Langmuir*, 2002, **18**, 1265-1269.
26. J. Guo and E. Lindner, *Anal. Chem.*, 2008, **81**, 130-138.
27. L. Su, F. Gao and L. Q. Mao, *Anal. Chem.*, 2006, **78**, 2651-2657.
28. A. J. Bard and L. R. Faulkner, *Electrochemical Methods, 2nd ed.; Wiley: New York*, 2001.
29. T. J. Davies and R. G. Compton, *J. Electroanal. Chem.*, 2005, **585**, 63-82.
30. B. Halliwell and J. M. C. Gutteridge, Free radicals in biology and medicine, *Oxford University Press*, New York, 2007.
31. (a) L. Q. Mao, K. Arihara, T. Sotomura and T. Ohsaka, *Chem. Commun.*, 2003, **22**, 2818-2819; (b) J. -i. Anzai, H. Takeshita, Y. Kobayashi, T. Osa and T. Hoshi, *Anal. Chem.*,

View Article Online
DOI: 10.1039/C6SM02791A

1998, **70**, 811-817.
32. F. Ricci and G. Palleschi, *Biosens. Bioelectron.*, 2005, **21**, 389-407.
33. (a) Z. J. Zheng, W. L. Daniel, L. R. Giam, F. W. Huo, A. J. Senesi, G. F. Zheng and C. A. Mirkin, *Angew. Chem. Int. Ed.*, 2009, **48**, 7626-7629; (b) F. Brinkmann, M. Hirtz, A. M. Greiner, M. Weschenfelder, B. Waterkotte, M. Bastmeyer and H. Fuchs, *Small*, 2013, **9**, 3266-3275; (c) X. Liao, K. A. Brown, A. L. Schmucker, G. L. Liu, S. He, W. Shim and C. A. Mirkin, *Nat. Commun.*, 2013, **4**, 2103; (d) K. A. Brown, D. J. Eichelsdoerfer, W. Shim, B. Rasin, B. Radha, X. Liao, A. L. Schmucker, G. L. Liu and C. A. Mirkin, *Proc. Natl. Acad. Sci. U.S.A.*, 2013, **110**, 12921-12924.
34. R. A. Potyrailo and V. M. Mirsky, *Chem. Rev.*, 2008, **108**, 770-813.

View Article Online
DOI: 10.1039/C6SM02791A

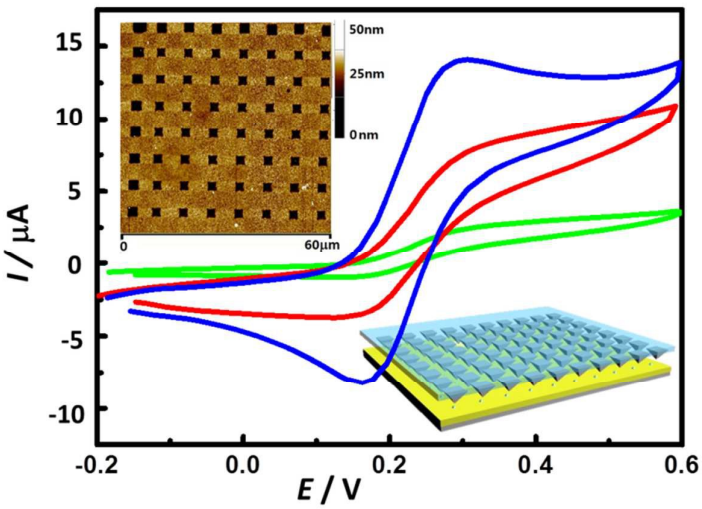

By combining polymer pen lithography with in-situ polymerization, we report a bottom-up approach for fabricating microelectrode arrays with well-controlled dimensions.